DEEP UV RAMAN AND CHEMICAL ANALYSIS OF CRYSTALLINE FELDSPAR AND PYROXENE IN POLYMICT MARTIAN METEORITE NORTHWEST AFRICA 10922: AN ANALOG STUDY FOR MARS 2020 SHERLOC AND PIXL AND MSL CHEMIN INSTRUMENTS.

R.V. Morris[1], N.C. Haney[2], R.S. Jakubek[2], S.A. Eckley[2], F.M. McCubbin[1], M.D. Fries[2], C.B. Agee[3], M.E. Schmidt[4], E.L. Berger[1], A. Yanchilina[5]. [1]NASA, Johnson Space Center, Houston, TX 77058. [2]Jacobs, NASA Johnson Space Center, Houston, TX 77058. [3]Inst. Meteoritics, Univ. New Mexico, Albuquerque, NM 87131. [4]Brock Univ., St. Catharines, ON, Canada. [5]Impossible Sensing, LLC, St. Louis, MO 63118.

Introduction: Martian meteorite Northwest Africa (NWA) 7034 and paired stones are polymict regolith breccias whose source lithologies date to ~4.4 Ga and major element compositions proximate average martian crust [1-3]. X-ray diffraction (XRD) mineralogy on a Northwest Africa (NWA) 7034 powder sample yielded plagioclase (~38%), alkali feldspars (~5%) low-Ca pyroxenes (~25%), clinopyroxenes (18%), Fe-oxides (10%), and apatite (~4%) with minor Fe-sulfide and chromite. [1]; [4] report similar results. The presence of crystalline feldspar, instead of XRD-amorphous and chemically equivalent maskelynite [e.g., 5], is attributed to low shock pressures during ejection from Mars [6, 7]. Feldspar chemical data for NWA 7034 and pairings are available [e.g., 8-10]. We report here chemical data and deep UV (DUV) Raman spectra for a slab of martian meteorite NWA 10922 (paired with NWA 7034) using laboratory analog instruments for the Mars 2020 PIXL and SHERLOC instruments [11-14] onboard the Perseverance rover. Our focus is feldspar, as NWA 7034 parings are unequivocal ground-truth samples for martian crystalline feldspar. The analogue-instrument methodology provides a PIXL-style identification of feldspar by chemistry and database spectra for SHERLOC-style DUV (248.6-nm excitation) Raman spectra. SHERLOC-style spectra were also acquired for terrestrial crystalline feldspar and terrestrial and martian-meteorite pyroxene samples.

Samples and Methods: The NWA 10922 slab (~4 cm diameter and ~4 mm thick from the Univ. New Mexico collection) was imaged for chemistry by µ-XRF (Bruker M4 TORNADO+; ~20 µm spot size). Element concentrations were not calibrated but were individually scaled to 100 count maximums. Element concentrations were organized into an image cube and concentration profiles made using ENVI software. DUV Raman spectra for the slab, <150 µm powders of labradorite, bytownite, orthoclase, and enstatite (from Oregon, Minnesota, Madagascar and Norway, respectively), and chips from two other martian meteorite (Elephant Moraine (EET) 79001 and Allan Hills (ALH) 84001)) were measured on ACRONM, a custom SHERLOC analog instrument at the Johnson Space Center with a ~50 µm spot size. For NWA 10922 ACRONM analyses, feldspar and pyroxene minerals were identified and located using µ-XRF and optical images, and relocated and Raman analyzed for at least three spots within each mineral grain.

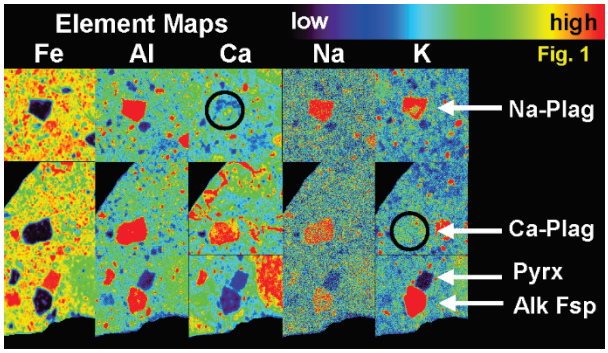

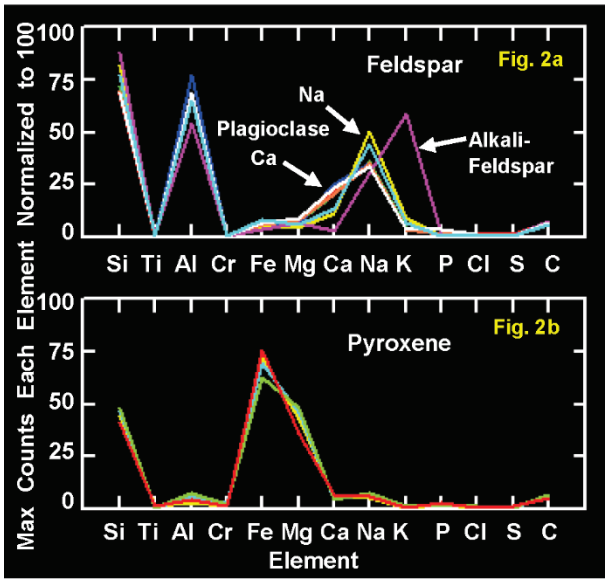

Discussion: NWA 10922 maps for 5 elements at three locations are shown in Fig. 1 (~5 mm x ~5 mm image dimensions). Feldspar (Al >> Fe) and pyroxene (Fe >> Al) minerals are recognized by

low (black) and high (red) Al and Fe concentrations. Feldspar minerals are differentiated by Ca, Na, and K with anorthitic plagioclase having Ca > (Na+K), albitic plagioclase having Ca < (Na+K), and alkali feldspar having K >> Ca.

Element profiles for 12 analyses readily distinguish feldspar (Fig. 2a) from pyroxene (Fig. 2b) and K-rich alkali feldspar from plagioclase. More subtle is differentiating albitic and anorthitic plagioclase, although differences in Ca and Na concentrations are evident (Fig. 2b).

Average plagioclase and the alkali feldspar DUV Raman spectra for NWA 10922 are plotted in Fig. 3a. We did not find a significant difference between average Raman spectra for the Ca > Na and Na > Ca plagioclase compositions (Fig. 3b). The feldspar Raman peaks at <600 cm^{-1} observed in ACRONM spectra are essentially not detectable in SHERLOC spectra because the latter has a Rayleigh rejection filter and a plasma emission line at ~654 cm^{-1} [13] and the former does not. ACRONM peaks at ~1600 cm^{-1} and broad humps at ~1370 cm^{-1} are assigned to macromolecular carbon (MMC) G and D bands, respectively. This leaves the shallow, broad hump centered near 1050 cm^{-1} as the sole SHERLOC-detectable feldspar feature. Reliable SHERLOC feldspar detection is enhanced by spectra with favorable combinations of high signal-to-noise ratios and absence of strongly absorbing phases in the same spectral region.

ACRONM feldspar spectra plotted in Fig. 3b show the "1050-feature" is likely a superposition of multiple (likely broad) bands having variable intensities. Specifically, orthoclase (alkali feldspar) is a doublet with peak centers near 998 and 1100 cm^{-1}; bytownite (plagioclase) has an asymmetric peak to longer wavenumbers and maximum intensity near 999 cm^{-1}; and labradorite (plagioclase) has a broad maximum centered near 1050 cm^{-1}. For NWA 10922 (Fig. 3a), it follows that the singlet (red) and doublet (cyan) profiles for their 1050-features imply plagioclase and alkali feldspar, respectively, in agreement with µ-XRF chemistry (Fig. 2).

Average ACRONM spectra for NWA 10922 pyroxene (Fig. 3c) are characterized by two pyroxene peaks at ~600 cm^{-1} and ~999 cm^{-1} and, like the feldspar spectra (Fig. 3a), the G and D bands from MMC. The positions of the pyroxene peaks are in family with those for terrestrial and other martian meteorite spectra (Fig. 3d). The Raman peak at ~1550 cm^{-1} (Fig. 3) results from atmospheric O_2 above sample surfaces.

Summary: Coupled µ-XRF and DUV Raman analyses on martian meteorite NWA 10922 and DUV Raman analysis on terrestrial plagioclase and alkali-feldspar minerals permit assignment of the shallow, broad spectra SHERLOC feature centered near 1050 cm^{-1} to crystalline feldspar as an alternative to "amorphous silicate" as proposed previously [15].

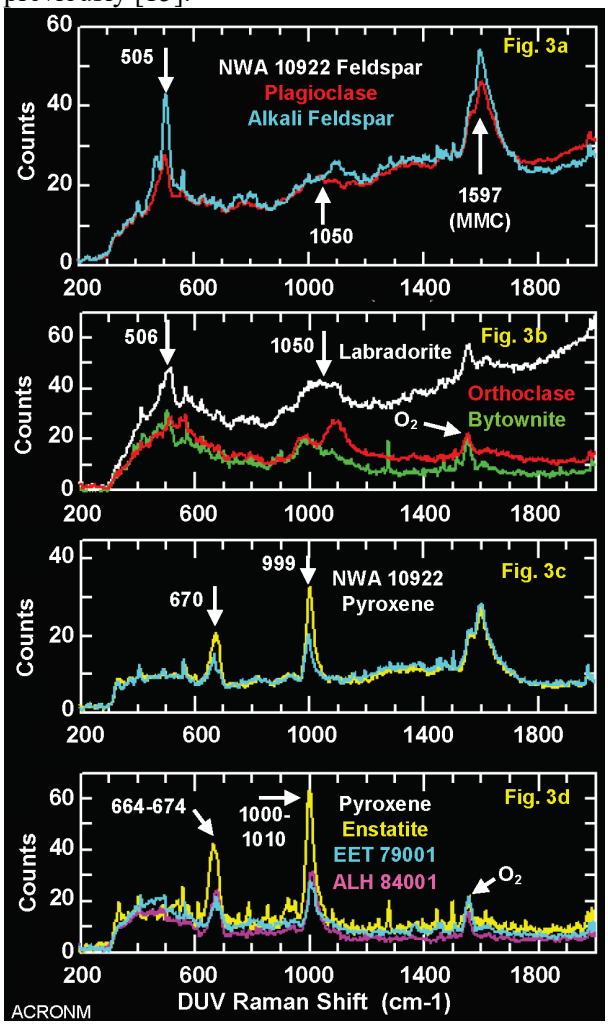

References: [1] Agee *et al.* (2013) *Science 339.* [2] McCubbin *et al.* (2016) *JGR-Planets 121*, 2120. [3] Cassata *et al.* (2018) *Sci. Adv. 4*:eaap8306. [4] Suga *et al.* (2019) *LPSC50*, abs#2000. [5] Papike *et al.* (2009) *GCA 73,* 7443. [6] Whittmann *et al.* (2015) *MAPS 50*, 326. [7] Leroux *et al.* (2016) *MAPS 51*, 932. [8] Santos *et al.* (2015) *GCA 157*, 56. [9] Santos *et al.* (2017) *LPSC48*, abs#2349. [10] MacArthur *et al.* (2019) *GCA 246,* 267. [11] Allwood *et al.* (2020) *SSR 216:134.* [12] Tice *et al.* (2022) *Sci. Adv. 8:47.* [13] Bhartia *et al.* (2021) *SSR 217:58.* [14] Fries *et al.* (2022) *SSR 218:46.* [15] Hollis *et al.* (2022) *Icarus 387,* 115179.